Development and Characterization of an Ionic Liquid Electrospray Thruster with a Porous Metal Blade Array

IEPC-2019-471

Presented at the 36th International Electric Propulsion Conference
University of Vienna • Vienna, Austria
September 15-20, 2019

Xinyu Liu[1] , Xiaoming Kang*[2], Weiguo He[3] and Qinqin Wu[4]
Shanghai Jiao Tong University, Shanghai 200240, China

Abstract: Ionic liquid electrospray thrusters, with advantages of high specific impulse, small volume and low power, have been considered as a promising propulsion option for nanosatellites. However, the thrust provided by one emission site of an electrospray thruster is small (10-100 nN) and therefore challenges are presented in scaling up the total emission currents with a good performance. This paper presents a miniaturized ionic liquid electrospray thruster using an array of sharp blades as emitter. The porous emitter array, integrated with seven 10 mm long sharp blades, is fabricated using wire electrical discharge machining (WEDM) combined with electrochemical etching. The propellant is passively fed to the emitter by capillary force so that the thruster configuration is compact and nonpressurized. The manufactured thruster is 30 mm×30 mm×17.5 mm in size and weighed less than 25 g. I-V test, time of flight (ToF) test, spatial plume distribution test and thrust test have been conducted in vacuum to characterize the performance of the thruster. Results show that the emitted current reaches 804 μA at +3000 V with a half plume angle of 60-70 degrees. Besides, when the applied voltage is 3000 V, the specific impulse of the electrospray thruster is estimated to be 1779.7 s and the thrust measures 77 μN.

Nomenclature

d	=	distance between the emitter and the extractor
f	=	current fraction
I_{sp}	=	specific impulse
I_{total}	=	total current
L	=	travelling distance of charged particles in ToF
m	=	mass of the emitted particles
$\dot{m}$	=	mass flow rate
q	=	charge of the emitted particles
r_p	=	radius of the pores of the porous material
R_t	=	apex curvature radius of the emitter
t	=	time of flight
T	=	thrust of the ionic liquid electrospray thruster
V_{app}	=	applied voltage
V_{start}	=	startup voltage of the thruster
γ	=	surface tension of the ionic liquid
ε_0	=	permittivity of vacuum

[1] Ph.D. candidate, School of Mechanical Engineering, liuxinyu@sjtu.edu.cn.
[2] Associate professor, School of Mechanical Engineering, xmkang@sjtu.edu.cn.
[3] Ph.D. candidate, School of Mechanical Engineering, Weiguo.He@sjtu.edu.cn.
[4] Master candidate, School of Mechanical Engineering, 61296114@qq.com.

I. Introduction

WITH the rapid development of space technology, human beings look to the vast space and trace the origin of the universe. As an important space technology, the artificial satellite technology has been paid attention to by all countries. At present, artificial satellites have become the largest number of spacecraft launched in the world. According to the mass, artificial satellites can be classified as large satellites (>1000 kg), medium satellites (500~1000 kg), small satellites (100~500 kg), micro satellites (10~100 kg), nano satellites (1 ~10 kg) and pico satellites (0.1 ~1 kg)[1]. And micro-nano satellites have become one of the main trends of satellite development due to the progress of microelectronic technologies and the consideration of development cost and launch difficulty. However, constrains of the volume, weight and power supply in micro-nano satellites bring great challenges to the development of propulsion system. Among the propulsion options for micro-nano satellites, ionic liquid electrospray thruster has been considered as a promising one since it has advantages of high specific impulse, small volume and low power[2].

Ionic liquid electrospray thruster is developed based on the electrospray phenomenon. Conductive fluids subjected to strong electric fields deform from a rounded shape into a conical structure and emit droplets, ions or a mixture of both[3], which is known as electrospray. Electrospray has been studied for more than one hundred years since the early 20^{th} century[4]. Colloid thruster is the early application of electrospray in space propulsion area[5-8]. In colloid thruster, doped organic solvent is utilized as the propellant. However, colloid thruster suffered from some issues such as high operating voltage, poor efficiency and difficulties in fabrication of capillary array. It is due to the development of chemical synthesis that new kinds of propellants—ionic liquids, were applied in electrospray. Ionic liquids are molten salts at room temperature which exhibit high electrical conductivities, low volatility and thermal stability[9]. In 2003, purely ion emission was first found by Romero-Sanz et al in the electrospray of 1-ethyl-3-methyl imidazolium tetrafluoroborate ($EMI\text{-}BF_4$). [10] Since then, the feasibility of ionic liquid electrospray thruster has been demonstrated in both laboratory investigations and flight testing[11-15].

Ionic liquid electrospray thruster consists of emitter, extractor, propellant feeding system and housing. Emitter is the key part of the ionic liquid electrospray thruster. It is responsible for amplifying the electric field and providing base for ion emission. Generally, there are three types of emitters: capillary emitters, externally wetted emitters, and porous emitters as shown in Fig. 1. The end of the emitter is terminated by an apex radius of several to tens of microns. One or several emission sites are based on the emitter end. However, the thrust provided by one emission site of an electrospray thruster is small[16] (~10-100 nN) and therefore challenges are presented in scaling up the total emission currents with a good performance. To solve this issue, linear or planar array of emitters are fabricated to increase the emission sites of the emitter[17-20].

This paper presents a miniaturized ionic liquid electrospray thruster using an array of sharp blades as emitter. The porous emitter array integrated with seven sharp blades is fabricated using wire electrical discharge machining (WEDM) combined with electrochemical etching. The propellant is passively fed to the emitter by capillary force so that the thruster configuration is compact and nonpressurized. I-V test, time of flight (ToF) test, spatial plume distribution test and thrust test have been conducted to characterize the performance of the thruster.

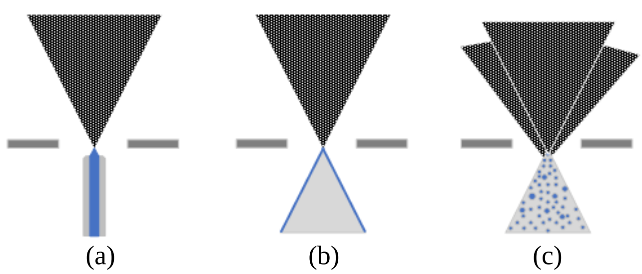

Figure 1. Three types of electrospray emitters: (a) capillary, (b) externally wetted and (c) porous.

II. Emitter Preparation and Thruster Fabrication

The schematic diagram of the designed thruster is depicted in Fig. 2. The emitter is a seven-blade array which integrated on a base. The adjacent blades are spaced by 2 mm and each of them is 10 mm long. The emitter array is prepared using WEDM combined with electrochemical etching. $EMI\text{-}BF_4$ is selected as propellant. The propellant is passively fed from the porous reservoir to the emitter by capillary force.

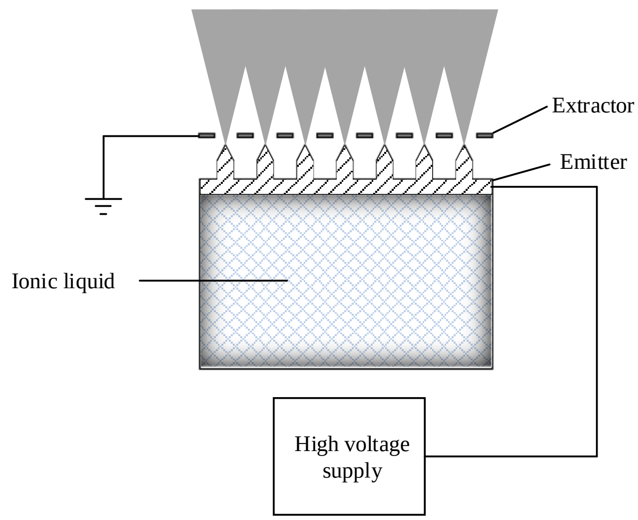

Figure 2. Schematic diagram of the designed ionic liquid electrospray thruster.

A. Emitter Preparation Process

The material of the emitter array is porous stainless steel with a mean pore size of 6 μm. The preparation of the emitter includes two processes: WEDM and electrochemical etching. The geometry of the emitter array is formed in the WEDM process outlined in Fig. 3. The WEDM process consists of the following steps:

a) The cuboid-shaped porous is clamped by the fixture and the cutting wire moves along the programmed path. The dark region of the material is removed and seven sharp blades are formed.

b) The fixture is rotated 90 ° and the edge of the emitter array is chamfered. The emitter array is cut off from the material.

c) The outer geometry of the emitter array is obtained.

After the WEDM process, an emitter array with seven sharp blades is obtained. However, the emitter cannot be directly used in the ionic liquid electrospray thruster. This is because a recast layer is formed on the machined surface during the WEDM process which will hinder the ionic liquid transportation. Thus, an additional electrochemical etching process is carried out to remove the recast layer. In the electrochemical reactions, the anode is the emitter array and a metallic ring serves as the cathode. The electrolyte is the phosphoric acid solution with a concentration of 7 M/L. The etching voltage is 5 V and the etching process lasts 40 s. After electrochemical etching, the emitter array are ultrasonic cleaned for more than 15 min to remove the acid solution attached to the emitter. The emitter array is observed by KEYENCE VHX-5000 digital microscope with a large depth-of-field and accurate measurement capabilities. The apex curvature radii of the blade range from 6 μm to 10 μm as shown in Fig. 4.

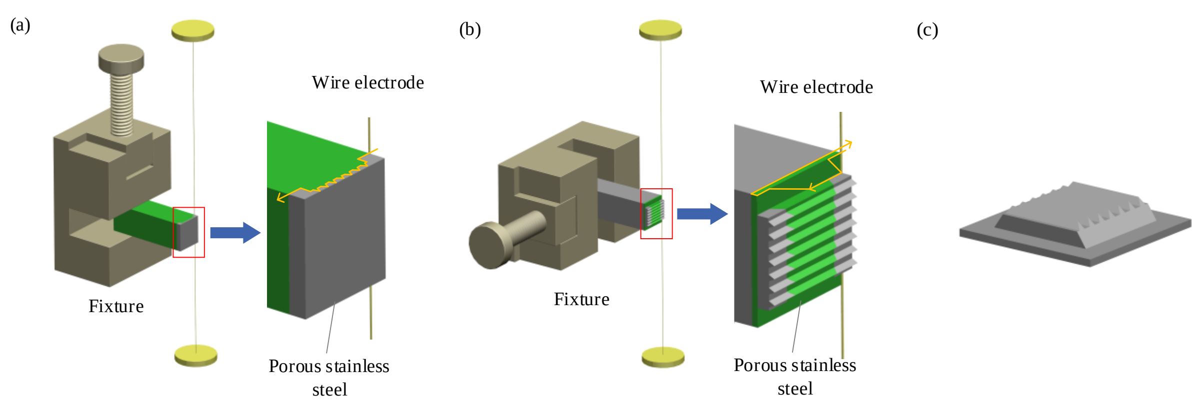

Figure 3. WEDM process of the emitter array: (a) cutting vertically, (b) chamfering and (c) machined emitter array.

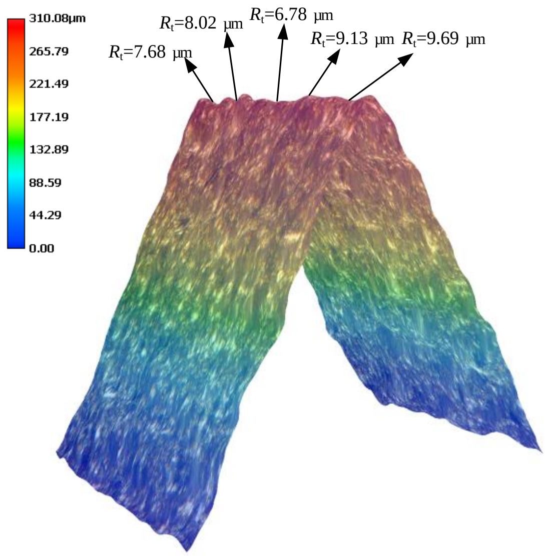

Figure 4. Observation of the emitter under the digital microscope.

B. Thruster Fabrication

The thruster consists of an emitter array, an extractor, a storage tank and housing. The extractor is laser cut from a 0.12 mm-thick stainless steel sheet. Seven linear extractor holes are 0.6 mm in width with a pitch distance of 2 mm. The storage tank is integrated with housing which is computerized numerical control (CNC) machined from a polyetheretherketone (PEEK) bulk. After wetted in the vacuum, the emitter array is assembled with the extractor and the housing through screw fastening. The emitter and the extractor hole are aligned with the aid of the microscope as shown in Fig. 5 (a). The distance gap between the emitter and the extractor is around 140 μm (the distance between the emitter end and the upper surface is about 260 μm). The assembled thruster measures 30 mm×30 mm×17.5 mm with a wet weight less than 25 g as shown in Fig. 5(b).

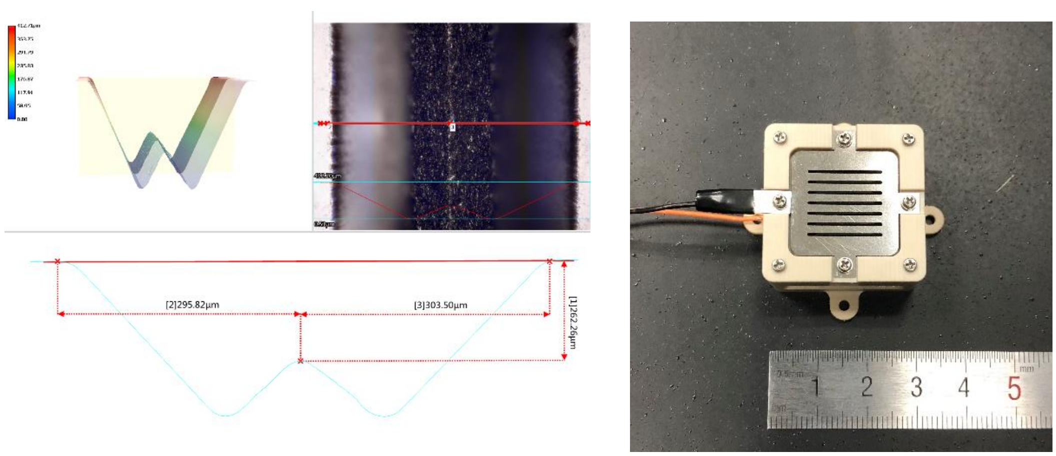

(a) (b)

Figure 5. Assembly of the ionic liquid electrospray thruster: (a) alignment under microscope and (b) the assembled thruster.

III. Experimental Apparatus

The experiments are conducted in a vacuum chamber in the State Key Laboratory of Mechanical System and Vibration in Shanghai Jiao Tong University. The chamber is 0.6 m in diameter and 1 m in length with two mechanical pumps, a roots pump and two turbo molecular pumps which can achieve a base pressure of 5×10^{-4} Pa.

A. I-V Characteristic Test

In the I-V characteristic test, high voltage supply is connected to the emitter and the extractor is grounded. Both the emitted current, which is the current drawn by the emitter from the high voltage supply, and the intercepted current, which is defined as the current measured from the extractor to ground, are obtained by measuring the voltage drop across a 1 kΩ resistor.

B. ToF Test

To measure the velocities of the emitted charged particles and further to determine the composition of the beam, time of flight (ToF) test is performed. The ToF setup includes electrostatic gate configuration, collector configuration and current signal acquisition configuration shown in Fig. 6. The electrostatic gate configuration comprising three highly transparent grids is placed 10 cm away from the extractor. The grid in the middle serves as electrostatic gate which is connected to high-voltage pulse, while the two grids adjacent to it are grounded. The potential of the pulse is a bit higher than the emitter potential so that the electrostatic gate configuration can interrupt the emitted charged particles. The collector configuration is installed 76.1 cm downstream from the electrostatic gate. The collector configuration consists of a grounded grid, succeeded by a bias grid to suppress secondary emission, and a collector plate. And the current signal acquisition configuration includes a current amplifier to amplify the current signal and an oscilloscope to record the current data.

When the potential of the electrostatic gate is switched to the high level, charged particles emitted later will be stopped by the gate, while charged particles which have got through the electrostatic gate will arrive at the collector plate after passing the potential free drift zone. Particles with different charge-to-mass ratios will gain different speeds after being accelerated by the same emitter potential. Thus, the time passing the distance between the electrostatic gate and the collector plate differs by the charge-to-mass ratio. The distribution of the charge-to-mass ratios can be obtained by analyzing the variation of the current collected by the collector plate.

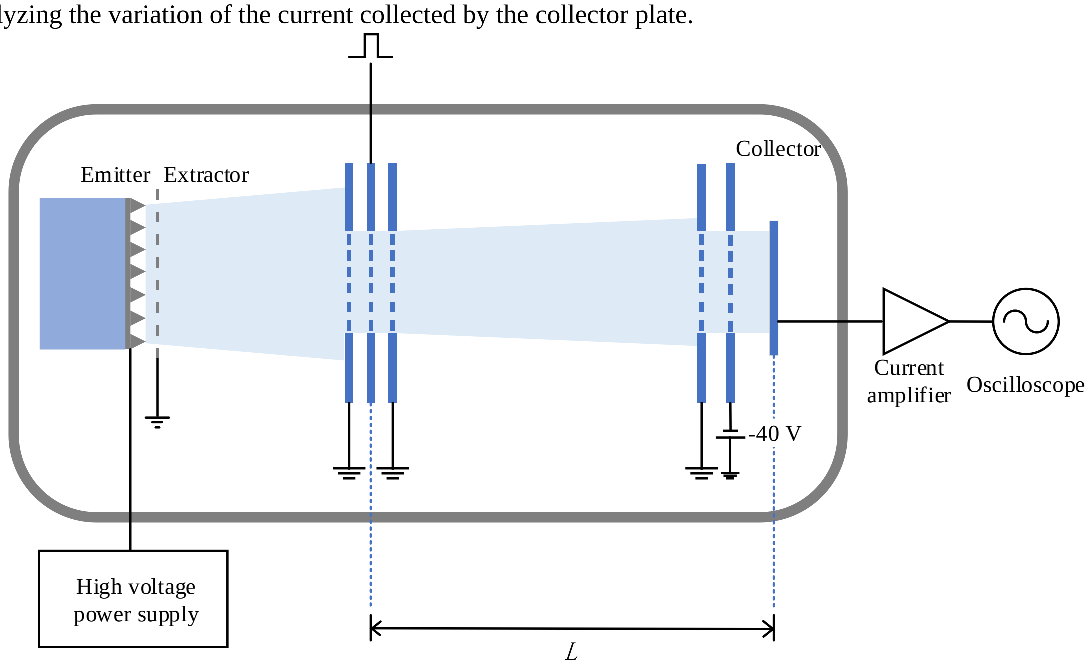

Figure 6. Schematic diagram of the ToF setup.

C. Spatial Plume Distribution Test

The spatial plume distribution is tested by measuring collected current when rotating the thruster either parallel to the blades or perpendicular to the blades as shown in Fig. 7. The ionic liquid electrospray thruster is installed on a rotating platform and the rotating shaft traverses the emission plane. The rotary motion of the platform is driven by a turbine worm mechanism connected to a stepper motor and the rotational speed can be regulated by the frequency of the pulse signal input. In the test, the rotational speed is set to 6 degrees per second. A barrier plate which is 300 mm×250 mm in size is mounted 65 mm downstream from the thruster. An aperture is on the center of the plate with a diameter of 6.3 mm. An 80 mm×80 mm metallic plate is set 75 mm away from the barrier plate to collect the charged particles passing the aperture. The thruster center, aperture center and the collector center are mounted coaxially.

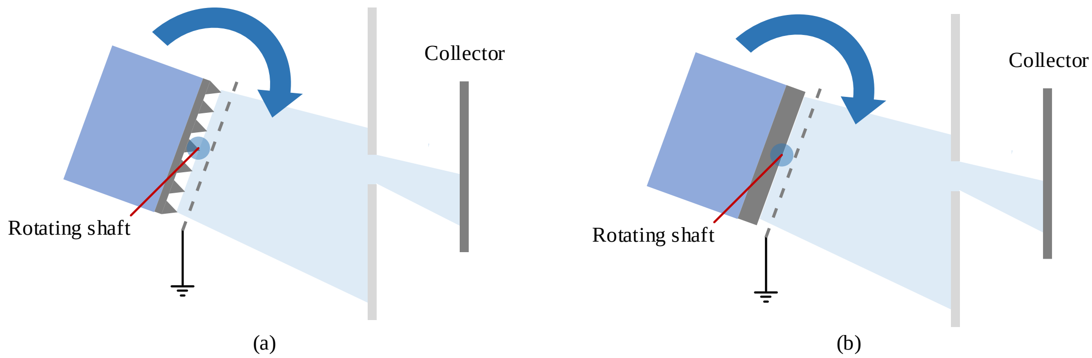

Figure 7. Schematic diagram of the spatial plume distribution setup: (a) rotating parallel to the emission blade and (b) rotating perpendicular to the emission blade.

D. Thrust Test

The thrust is measured directly via a high-precision mass balance module. The test schematic diagram is shown in Fig. 8. A high-precision mass balance, with a resolution of 0.1mg (equivalent to ~1 μN of force), is installed to the vacuum chamber. The ionic liquid electrospray thruster is fixed on the weighing plate of the mass balance so that the charged particles are emitted upwards. Before testing, the mass balance has been calibrated by both external calibration and internal software calibration. It should be noted that the pressure of the vacuum chamber should be pumped to a constant value and the reading of the weight must keep constant before firing.

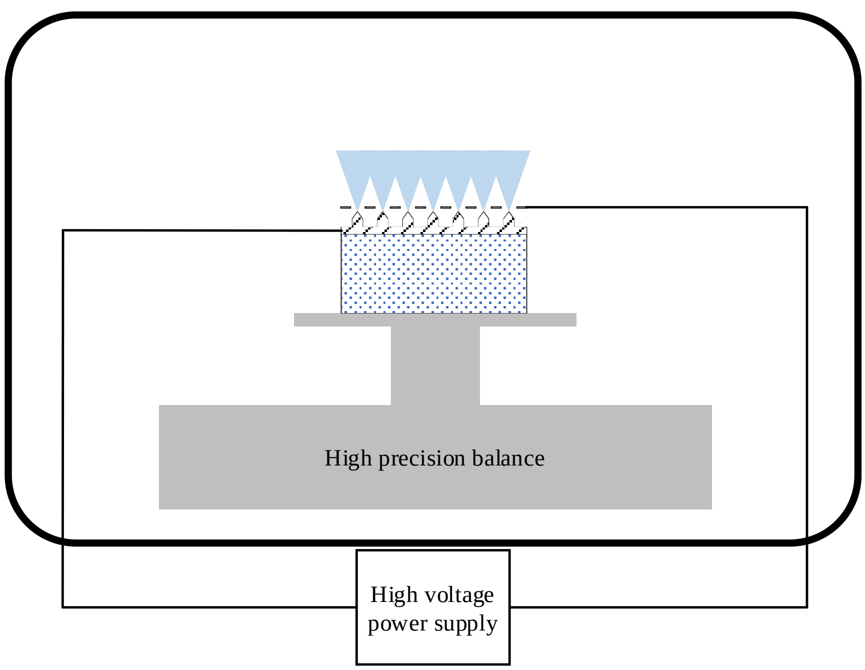

Figure 8. Schematic diagram of the thrust measurement setup.

IV. Results and Discussion

A. I-V Characteristic Test

The variation of both emitted current and the intercepted current with the applied voltage is shown in Fig. 9. The startup voltage, which is defined as the minimum voltage that starts an electrospray emission, is 1280 V. Apart from the experimental value, the startup voltage can also be estimated by the following equation[21]

$$V_{\text{start}} \sim \sqrt{\frac{\pi\gamma R_{\text{t}}^2}{8\varepsilon_0 r_{\text{p}}}} \ln\left(\frac{4d}{R_{\text{t}}}\right) \tag{1}$$

Given that the apex curvature radii and pore size fluctuate in a range, accurate estimation of the startup voltage is not expected. Here, we take some typical values in the range to calculate the startup voltage. When γ = 45.2 mN/m, d = 140 µm, r_{p} =3 µm and R_{t} = 9 µm, the calculated startup voltage is 1217 V with an error of 4.9 % compared with the experimental value.

Both the emitted current and the intercepted current grows with the increase of the applied voltage. In the positive polarity, the curve is similar to be quadratic from the startup voltage to 2500V while it is similar to be linear form 2500 V to 3000 V. The emitted current reaches 804 µA at +3000 V and -790 µA at -3060 V. And the intercepted current is within 6 % of the emitted current.

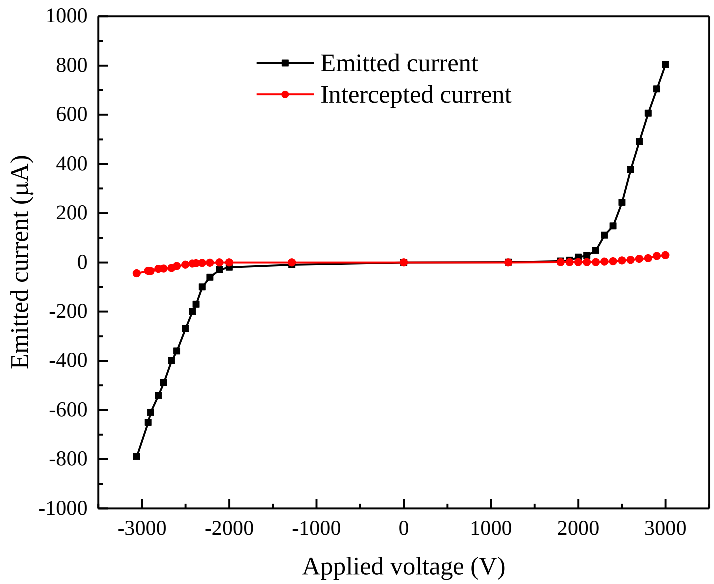

Figure 9. I-V characteristic curve of the ionic liquid electrospray thruster.

B. ToF Test

Fig. 10 illustrates the typical ToF traces for the EMI-BF_4 at 3000 V applied voltage. The current steps in 10.57 µs and 17.63 µs indicate the existence of both monomer and dimmer. Assuming all evaporated ions are singly charged and ignoring fragmentation, the mass flow rate is estimated as follows

$$\dot{m} = I_{\text{total}} \cdot \sum_i \frac{f_i}{(q/m)_i} \tag{2}$$

In the ToF test, high-speed charged particles travel a distance L. The current fractions are measured by averaging the relative magnitudes of the respective current steps. Ignoring the thruster efficiency, the ideal specific impulse are then computed from the ToF as

$$I_{\text{sp}} = \frac{\sum_i \dot{m}_{\text{i}} (L/t)_i}{\dot{m} g} \tag{3}$$

The ideal specific impulse at 3000 V is calculated to be 4943.6 s. It should be noted that the ideal value is much larger than the practical value. Taking the total efficiency of 36 % in Ref. 14 into consideration, the specific impulse is estimated to decrease to 1779.7 s.

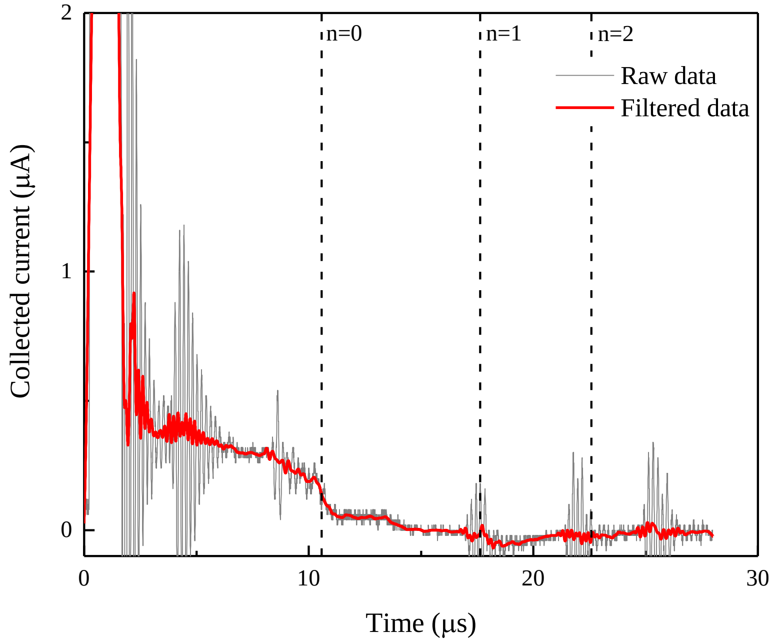

Figure 10. ToF traces for the EMI-BF4 at 3000 V.

C. Plume Spatial Distribution Test

Fig. 11 shows the normalized collected current at an applied voltage of +3000 V versus rotation angle with the axis of rotation orientated parallel and perpendicular to the emission blades. The maximum half-angle of the plume is approximately 60-70 degrees. Compared with being rotated perpendicular to the emission blades, the shape of the plume curve has three peaks when the rotation axis is parallel to the blades. This is probably caused by superposition of multiple ion beams emitted from different emission blades.

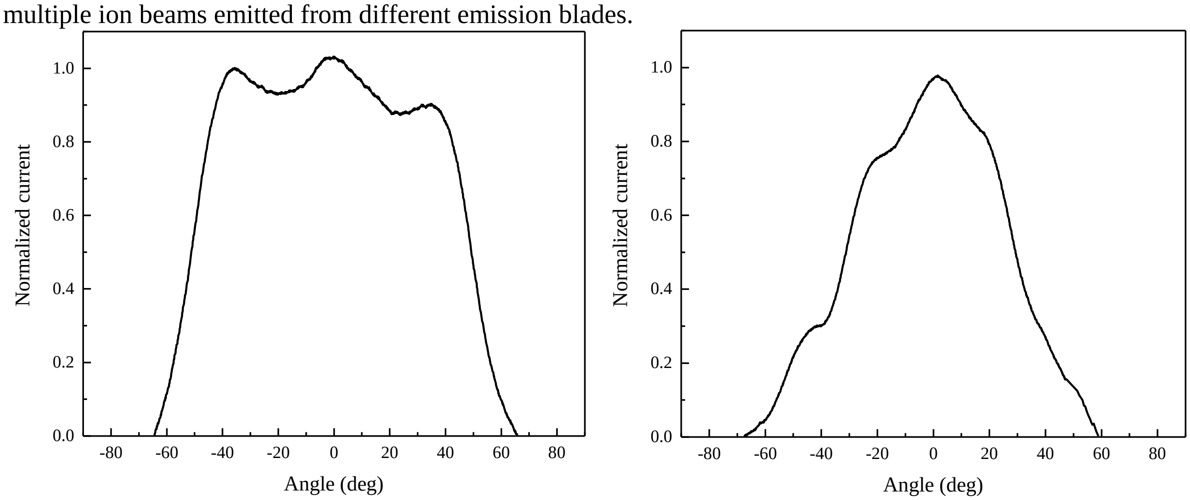

(a) (b)

Figure 11. Plume spatial distribution: (a) rotating parallel to the emission blade and (b) rotating perpendicular to the emission blade.

D. Thrust Test

A series of thrust measurements at different applied voltages have been conducted and the measured thrust is shown in Fig. 12. The thrust increases from 2 μN to 77 μN when the applied voltage is adjusted from 2100 V to 3000 V.

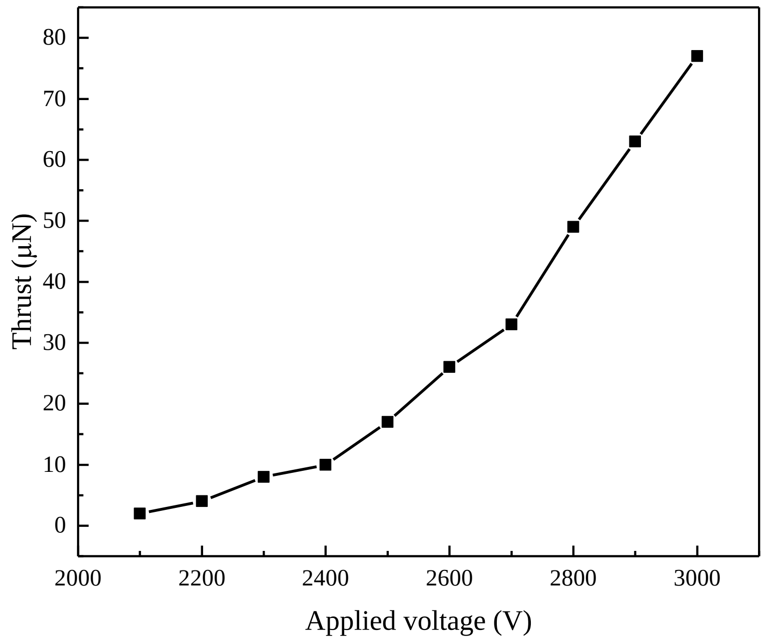

Figure 12. Variation of the measured thrust versus applied voltage.

V. Conclusion

An ionic liquid electrospray thruster with a porous metal blade array is developed. The propellant is passively fed to the emitter so that the structure is compact (30 mm×30 mm×17.5 mm in size) and the weight is light (with a wet weight less than 25 g). The porous metal blade array is prepared by WEDM followed by electrochemical etching. The apex curvature radii of the fabricated emission blade range from 6 μm to 10 μm. To characterize the developed thruster, I-V characteristic test, ToF test, spatial plume distribution test and thrust test have been conducted. Results indicate that the emitted current reaches 804 μA at +3000 V and the intercepted current is less than 6 % of the emitted current. Besides, the maximum half-angle of the plume is 60-70 degrees. The specific impulse is estimated to be 1779.7 s and the measured thrust is up to 77 μN at 3000 V.

Acknowledgments

The research is supported by the National Natural Science Foundation of China (Grant No.51675341).

References

[1]Barnhart, D. J., Vladimirova, T., and Sweeting, M. N., “Satellite-on-a-Chip development for future distributed space missions,” *Proceedings of the CANEUS 2006: MNT for Aerospace Applications*, CANEUS2006-11045, ASME, Toulouse, 2006, pp. 199-212.

[2]Lozano, P. C., Wardle, B. L., Moloney, P., and Rawal, S., “Nanoengineered thrusters for the next giant leap in space exploration,” *MRS Bulletin*, Vol. 40, No. 10, 2015 ,pp. 842-849.

[3]Chiarot, P. R., Sullivan, P., and Mrad, R. B., “An overview of electrospray applications in MEMS and microfluidic systems,” *Journal of Microelectromechanical Systems*, Vol. 20, No. 6, 2011, pp. 1241-1249.

[4]Zeleny, J., “Instability of electrified liquid surfaces,” *Physical review*, Vol. 10, No. 1, 1917, pp. 1-6.

[5]Kidd, P. W., “Parametric studies with a single-needle colloid thruster”, *Journal of Spacecraft and Rockets*, Vol. 5, No. 9, 1968, pp. 1034-1039.

[6]Mahoney, J. F., Moore, R. D., Perel, J., and Yahiku, A. Y., “Research and development of a charged-particle bipolar thruster,” *AIAA Journal*, Vol. 7, No. 3, pp. 507-511.

[7]Bailey, A. G., “Investigation of a single spraying site of a colloid thruster,” *Journal of Physics D: Applied Physics*, Vol. 6, No. 2, 1973, pp. 276.

[8]Huberman, M. N., and Rosen, S. G., “Advanced high-thrust colloid sources,” *Journal of Spacecraft and Rockets*, Vol. 11, No. 7, 1974, pp. 475-480.

[9]Prince, B. D., Fritz, B. A., and Chiu, Y. H., “Ionic Liquids in Electrospray Propulsion Systems,” *Ionic Liquids: Science and Applications*, ACS Symposium Series, American Chemical Society, Washington, DC, 2012, Vol. 1117, Chaps. 2, pp. 27-49.

[10]Romero-Sanz, I., Bocanegra, R., Fernandez De La Mora, J., and Gamero-Castano, M., “Source of heavy molecular ions based on Taylor cones of ionic liquids operating in the pure ion evaporation regime,” *Journal of Applied Physics*, Vol. 94, No. 5, 2003, pp. 3599-3605.

[11]Lozano, P., and Martinez-Sanchez, M., “Ionic liquid ion sources: characterization of externally wetted emitters,” *Journal of colloid and interface science*, Vol. 282, No. 2, 2005, pp. 415-421.

[12]Lenguito, G., and Gomez, A., “Development of a multiplexed electrospray micro-thruster with post-acceleration and beam containment,” *Journal of Applied Physics*, Vol. 114, No. 15, 2013, 154901.

[13]Dandavino, S., Ataman, C., Ryan, C. N., Chakraborty, S., Courtney, D., Stark, J. P. W., and Shea, H., “Microfabricated electrospray emitter arrays with integrated extractor and accelerator electrodes for the propulsion of small spacecraft,” *Journal of Micromechanics and Microengineering*, Vol. 24, No. 7, 2014, 075011.

[14]Demmons, N. R., Lamarre, N., Ziemer, J. K., Parker, M., and Spence, D., “Electrospray thruster propellant feed system for a gravity wave observatory mission”, *52nd AIAA/SAE/ASEE Joint Propulsion Conference*, AIAA-2016-4379, AIAA, Salt Lake City, 2016.

[15]Krejci, D., Mier-Hicks, F., Thomas, R., Haag, T., and Lozano, P., “Emission characteristics of passively fed electrospray microthrusters with propellant reservoirs,” *Journal of Spacecraft and Rockets*, Vol. 54, No. 2, 2017, pp. 447-458.

[16]Courtney, D. G., Dandavino, S., and Shea, H., “Comparing direct and indirect thrust measurements from passively fed ionic electrospray thrusters,” *Journal of Propulsion and Power*, Vol. 32, No. 2, 2016, pp. 392-407.

[17]Legge, R. S., and Lozano, P. C., “Electrospray propulsion based on emitters microfabricated in porous metals,” *Journal of Propulsion and Power*, Vol. 27, No. 2, 2011, pp. 485-495.

[18]Courtney, D. G., Li, H., and Lozano, P. C., “Electrochemical micromachining on porous nickel for arrays of electrospray ion emitters,” *Journal of Microelectromechanical Systems*, Vol. 22, No. 2, 2012, 471-482.

[19]Lenguito, G., De La Mora, J. F., and Gomez, A., “Scaling up the power of an electrospray microthruster,” *Journal of Micromechanics and Microengineering*, Vol. 24, No. 5, 2014, 055003.

[20]Courtney, D., Dandavino, S., & Shea, H., “Performance and Applications of Ionic Electrospray Micro-Propulsion Prototypes,” *AIAA SPACE 2015 Conference and Exposition*, AIAA-2015-4672, AIAA, Pasadena, 2015.

[21]Courtney, D. G., Li, H. Q., and Lozano, P., “Emission measurements from planar arrays of porous ionic liquid ion sources,” *Journal of Physics D: Applied Physics*, Vol. 45, No. 48, 2012, 485203.